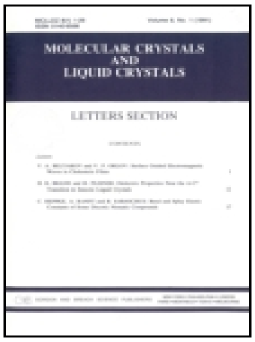
MOLECULAR CRYSTALS AND LIQUID CRYSTALS

LETTERS SECTION

Molecular Crystals and Liquid Crystals

ISSN: 1542-1406 (Print) 1563-5287 (Online) Journal homepage: http://www.tandfonline.com/loi/gmcl20

Effect of Polarization on Recombination of Charge States in an Ionizing Particle Track in Organic Molecular Crystals

Nikolai Z. Galunov & Oleg A. Tarasenko

To cite this article: Nikolai Z. Galunov & Oleg A. Tarasenko (2015) Effect of Polarization on Recombination of Charge States in an Ionizing Particle Track in Organic Molecular Crystals, Molecular Crystals and Liquid Crystals, 606:1, 176-188, DOI: 10.1080/15421406.2014.905051

To link to this article: http://dx.doi.org/10.1080/15421406.2014.905051

Mol. Cryst. Liq. Cryst., Vol. 606: pp. 176–188, 2015
Copyright © Taylor & Francis Group, LLC
ISSN: 1542-1406 print/1563-5287 online
DOI: 10.1080/15421406.2014.905051

Effect of Polarization on Recombination of Charge States in an Ionizing Particle Track in Organic Molecular Crystals

NIKOLAI Z. GALUNOV AND OLEG A. TARASENKO*

Institute for Scintillation Materials of NAS of Ukraine, Kharkov, Ukraine

The effect of polarization on the energy exchange of charge states in molecular media is studied for the case when no external electric field exists. Measurements of the light yield of organic molecular crystals excited by ionizing radiations are used to verify theoretical hypotheses. This allows us to carry out experiments for a wide range of the initial density of charge states. The polarization process initiates the primary recombination of hot carriers those are generated in the particle track. This reduces the radioluminescence (RL) energy yield of organic molecular crystals with increasing the specific energy loss of an ionizing particle.

Keywords Charge state; energy yield; organic crystal; polarization; radioluminescence

Introduction

Organic molecular crystals, as organic molecular solids in general, have unique optical and electronic properties. Molecules in organic crystals are bonded by the van der Waals forces [1–6]. The energy of these interactions is 10^3 times less than the energy of covalent interactions between atoms in a molecule [2, 4]. Huge quantitative differences in the energies of the lattice interactions in organic molecular and inorganic covalent (ionic) crystals cause qualitative differences in the formation and transport of excess charge carriers. The energy structure of molecular crystals and electronic processes in them are defined both supramolecular and electronic structure of the molecules that make up a crystal. Delocalized and weakly bonded π-electrons of conjugation of the molecules of aromatic hydrocarbons and n-electrons of conjugated heterocyclic compounds are a potential source of the formation of charge carriers under the light, temperature, external field, or ionizing radiation [1–3].

Weak intermolecular forces are responsible for a strong localization of a charge carrier. It moves by incoherent hops in an organic molecular crystal [2]. At high temperatures, charge carriers due to their pronounced localization on individual molecules during their motion have time to interact strongly with the electronic and nuclear subsystems, and, in some cases, with the lattice subsystem of the environment. It causes formation of electronic, molecular, and lattice polarons, respectively. The electronic polaron formation results in

---

*Address correspondence to Oleg A. Tarasenko, Code: 61001, Institute for Scintillation Materials of NAS of Ukraine, 60 Lenin av., Kharkov, Ukraine. Tel.: +380 57 3410259; Fax: +380 57 3404474. E-mail: tarasenko@isma.kharkov.ua increase of intermolecular energy to 10^{-1} eV. This energy is by a factor of 10^2 greater than the energy of the van der Waals interactions that hold molecules in a crystal [2, 4].

Organic molecular crystals due to the above-discussed features of their structure and specific electronic properties are widely used as semiconductors, light-emitting diodes, elements of nonlinear optics, and detectors of ionizing radiations [1–7]. Different applications have their own aspects. For example, a powerful external electric field is not used during experiments in the scintillation applications. In this case, the energy exchange of charge states is determined by the internal electric fields occurring between molecules with electron deficiency and excess. Note that the formation of particle tracks can be corresponded to the extreme case of extra-large initial concentrations of charge states. In itself, this is a very interesting scientific problem.

The organic single crystals used as efficient scintillators have a monoclinic structure with close values of parameters of the unit cell, with the densities close to 1.2 g/cm^3, and the similar values of the effective atomic number and effective nuclear charge [8]. The single crystals of anthracene, stilbene, and *p*-terphenyl [4, 7, 9–12] are the most applicable organic scintillation crystals. In the latter case, the single crystals with and without a dopant of 0.1% 1,4-diphenyl-1,3-butadiene in the melt are used [4, 10]. Organic molecular scintillation crystals are often used for detection of the ionizing radiations, which have high specific energy loss (dE/dx) [4, 7].

In this paper we analyze the energy exchange of charge states in the high activation density regions of the quasi-spherical (spurs) and quasi-cylindrical (tracks) symmetry on the hypothesis that the influence of the polarization interactions is of primary importance [13]. It is should be noted that the influence of polarization effects was earlier discussed in the context of the mechanisms of the fast component formation of the radioluminescence (RL) pulse in regions of the low activation density of organic molecular solids and liquids [9, 14–16]. Therefore, the discussion of this material is beyond the scope of this paper.

Theory

Aspects of Charge State Generation in an Organic Molecular Medium

Ionizing radiations generate excess charge carriers in an organic molecular crystal [1]. In this case, a quasi-free electron rapidly localizes on some other molecule and produces a negative quasi-ion M_-. The molecule, which has lost an electron, becomes a positive quasi-ion M_+. A displacement of π-orbitals and positively charged molecules occurs in different directions in the surrounding of the molecular quasi-ion. The polarization surrounding originates including about 10^3 molecules. The electronic polarons $M_p{}^-$ and $M_p{}^+$ are formed around the quasi-ions M_- and M_-, respectively [2]. The energy of the electrostatic field of a quasi-ion E_{pol} that is necessary to create the polarization surrounding is about 1–1.5 eV. The polarization time of the electron orbitals of the molecules of an organic crystal is estimated as $\tau_e \approx 10^{-16}$–10^{-15} s. The electrostatic field of the quasi-ions disappears as the result of a pair recombination of M_+ and M_-. Directly after this, π-orbitals and positively charged skeletons of molecules, which had been polarized by the electrical field of the M_+ and M_- pair, return to equilibrium giving off the vibrational energy. This energy corresponds to the energy, which is spent for their initial displacement during the formation of the polarization surrounding [2, 4]. Besides, the formation of the molecular exciton localized at high temperatures on the molecule, which was a quasi-ion before the recombination, becomes possible. The relation between the probabilities of the exciton decay with and without the emission of a light photon (the energy E_{ph} is about 3 eV [4]) determines the RL intensity. The ratio of the energy of the emitted light to the energy of an ionizing radiation accumulated in a crystal, determines the energy yield of the scintillation process. This yield can be different for different types of ionizing radiations.

If the distance d between the charge states ${M_p}^+$ and ${M_p}^-$ is less than the value of the radius of the stable polarization surrounding r_c (1), then a pair of molecular polarons forms [2, 4]. The value of r_c is defined as [2]:

$$r_c = \frac{e^2}{4\pi \ \langle \varepsilon \rangle \ \varepsilon_0 \, k \, T}, \tag{1}$$

where $\langle \varepsilon \rangle$ is an average relative permittivity of a crystal, k is the Boltzmann constant, T is a temperature, and ε_0 is the dielectric constant.

The value of the local field strength E_{loc} that created by a pair of charge states ${M_p}^+$ and ${M_p}^-$, localized on different lattice sites, will vary depending on the distance between ${M_p}^+$ and ${M_p}^-$. It is easy to obtain the following estimates using the data [17]. For example, for the single crystal of anthracene the values of E_{loc} created by such a pair are in the range from 1.8×10^6 to 3.2×10^7 V/cm when the distance d changes from r_c to the distance between the nearest neighbor molecules. These values exceed the breakdown voltage of organic crystals [1]. According to [2, 4] in such a case the charge carrier scattering time τ becomes a very small quantity that is less than 10^{-13} s. According to [18], the thermalization time of charge carriers in these systems is by an order of magnitude greater. The strong local electric fields inside such the pair have to increase the probability of the recombination of hot charge states, especially, when no an external electric field is applied [1]. The contribution to the total recombination process of the very fast initial recombination of the hot charge state pairs should increase with their concentration.

During the excitation by an ionizing particle in each a single event of interaction with a medium this particle mainly transmits such a portion of it energy, which exceeds the ionization potential of molecules. The ionizing radiations with low values of $\mathrm{d}E/\mathrm{d}x$ ($<10^1$ MeV/cm), such as electrons with energies above 100 eV, photons of gamma radiation (that generate secondary electrons in an organic medium) create separate local regions of excitation (spurs). These regions do not overlap. The ionizing radiations with values of $\mathrm{d}E/\mathrm{d}x \geq 10^1$ MeV/cm (protons, alpha particles, heavy ions) generate the spurs those overlap and form a single region of high activation density, i.e. the particle track [4, 19]. Generation of charge states in the ionizing particle track proceeds through a rapid (10^{-16}–10^{-15} s [4]) initial stage of a decay of superexcited [20] and plasmon states [1, 4, 21–23]. Fano [23] considered organic molecular systems as the most obvious example of systems in which the generation of plasma oscillations was possible. According to the experimental data the average energy of plasmons in organic condensed media is estimated as $\langle E_{\mathrm{pl}} \rangle \sim 20$ eV [1, 4, 13, 21, 22].

It is known that the probability of the nonradiative decay of a molecular exciton increases with increasing temperature, while the probability of luminescence decreases [24]. During the simultaneous recombination of j polaron pairs the vibration energy, which is comparable to or lower than the energy of the lowest singlet excited state S_1, should be released. It means that the probability of the nonradiative losses must increase with increasing $\mathrm{d}E/\mathrm{d}x$, i.e. with increasing j. As a result, the RL energy yield should decrease with an increase in the j-value. Such a change can be correctly examined by the measurements of the RL light yield.

The Model Representation of Tracks and Spurs as Volumes with the Cylindrical and Spherical Symmetry, Respectively

Despite of an evident disagreement between the real processes and the approach, which considers tracks (spurs) as the volumes of a cylindrical (spherical) symmetry with the "sharp" boundaries, this approach is successfully used since the time of the investigation of particle tracks in the cloud chamber [1, 4, 7, 19]. This approach allows us to introduce the definition of the initial radius r_0 of a cylindrical track or a spherical spur. It gives a possibility to carry out not only some estimations, but to make quantitative calculations as well. This approach means the following.

The Gaussian distribution of the initial concentration of charge pairs (in the plane perpendicular to a cylinder axis, or in the cross-section of a sphere passing through two of its diameter) is replaced by the truncated Gaussian distribution. This distribution ignores the presence of a small number of the pairs that are on the distances larger then a diameter of a cross-section of such the cylinder. In this case, the diffusion-controlled process of annihilation of triplet excitons (T-states) in the region of a track (or a spur) can lead to the generation of S_1-states, which results in a rise of the number of RL photons [1, 14–16]. A time t of such a photon appearance after excitation is additionally delayed on the time required for two triplet excitons to meet each other. The delayed RL forms the slow component of a scintillation pulse. Its shape can be described as [4, 16]:

$$I(t) \approx (1 + (t/t_D))^{-k}, \tag{2}$$

where Eq. (3) defines the time of a diffusion expansion of the track (spur) t_D in the medium with the diffusion coefficient D of T-states. The value k is equal to 1.0 or 1.5 for the high excitation density regions with the cylindrical or spherical symmetry, respectively:

$$t_D = r_0^2/4D. \tag{3}$$

Experimental checking the k-values for the wide class of organic scintillators (from liquids to single crystals) gives the following results for $t > 50$ ns. The condition $k = 1.0$ is satisfied with an accuracy no greater than 5–6% in the case of the excitations by alpha particles and fast neutrons (that create recoil protons). For the excitations by conversion electrons or photons of gamma radiation the condition $k = 1.5$ is satisfied with an accuracy of 7–8% [4]. It also means that in the first case the tracks are essentially formed, while in the second case the spurs are formed. These results explain why the application of the discussed approach in radiation chemistry, radiation physics, and scintillation technique is so successful [1, 4, 7, 19].

The second very important result of the discussed studies is the following. Equation (2) describes the diffusion-controlled process for $t > 50$ ns [4]. It means that the main energy losses in the scintillation process have to occur in the earlier times after an excitation.

The Semi-Empirical Description of the Energy Exchange Processes of Charge States in Organic Crystals for High Excitation Densities

Recently [25], we proposed the semi-empirical description of the primary energy exchange in the ionizing particle track with the cylindrical symmetry that takes into account the polarization interactions in organic molecular media. It was shown that the rates, which describe the probabilities of the primary fast recombination of hot charge state pairs in the track, and the rates, which describe the pair recombination of those charge states that in the initial time are at a distance that exceeds r_c (1), appear in the final equation with the opposite signs. In the former case the hot charge states ${M_p}^+$ and ${M_p}^-$ are on very short distances. The probability of a simultaneous recombination of more than one the pair becomes high. In the latter case, the additional time is necessary to the charge states to approach each other within the distance less than r_c (1). They have a time to relax to the molecular polarons. The probability of a simultaneous recombination of more then one of such the pairs in a very small volume is negligible.

In [13, 26] the detailed analysis of this description was performed. In particular, it was obtained the following results. The influence of the type and structure perfection of a scintillator on losses in the light yield is not as important as the influence of the processes of the primary quenching inside the ionizing particle track. With increase of the initial concentration of charge states the quenching effect grows. It is the primary quenching that has to be the concentration-controlled process [13]. With an increase of the initial concentration of charge states, the fraction of polarons, which take part in the primary recombination, grows. This has to cause the increase of the quenching effect, i.e. the decrease of the number of RL photons [26].

The Recombination of Charge State Pairs for the Case of Excitation with High dE/dx

If the above-mentioned analysis is correct, then the probability of the primary recombination of hot charge states should depend on the relation between r_c (1) and the average initial distance d between charge states. This distance will be determined by dE/dx, and hence by the type of an excitation. Therefore, to revise the results of the analysis it is necessary to calculate the values of r_c and d for different types of crystals and irradiations. The calculations of r_c (1) for a number of organic single crystals were carried out in [27]. The r_c-values were in the range from 15.4 nm for the single crystal of stilbene to 19.5 nm for the single crystal of *p*-terphenyl. We calculated the d-values for the single crystals of anthracene, stilbene, and *p*-terphenyl excited by alpha particles, fast neutrons and electrons. The results obtained for different single crystals had no a qualitative difference. For alpha particles, it was obtained that $d < r_c$, for electrons and photons of gamma radiation of the medium energies the relation $d > r_c$ was correct. For the case of the excitation by fast neutrons of different energies, both cases could be observed. For $d > r_c$, in contrast to $d < r_c$, the polarization surroundings of neighbor pairs do not overlap. It means that in the case of the excitation by a fast neutron the influence of the polarization effects on the fast recombination of hot charge states should not be as strong as in the case of the excitation by an alpha particle.

The Experimental Studies of the Recombination Process of Charge State Pairs for a High Excitation Density

The data that were discussed in the section "Theory" are in a good agreement with the hypothesis that the fast initial quenching effect is caused by the primary recombination of hot charge states and increases with these states concentration. If this hypothesis is correct, then the energy yield of the scintillation process has to decrease with increasing the initial concentration of charge pairs, or with increasing dE/dx of a particle. In this formulation, the problem can be directly solved on a base of the measurements of the scintillation light yield for a wide range of dE/dx values.

Experimental

Radionuclide Sources

To obtain a wide range of dE/dx we used medium energy photons of gamma radiation with energies $E_\gamma \sim 10^5$–10^6 eV (^{22}Na, ^{60}Co, ^{137}Cs, and ^{152}Eu radionuclide sources), conversion electrons with the energy $E_e = 0.622$ MeV (the ^{137}Cs source), alpha particles in the energy range from 0.7 to 7.5 MeV, fast neutrons from a ^{239}Pu-Be source.

The alpha particles for such the energy range were obtained by attenuation of alpha particles from ^{239}Pu (5.15 MeV) and ^{226}Ra (7.68 MeV) isotopes in a layer of air. The actual energies of the alpha particles were estimated from their residual range [4].

To separate the spectrum of recoil protons generated by fast neutrons of a ^{239}Pu-Be radionuclide source in organic crystal, we used the method of discrimination of an ionizing radiation by a scintillation pulse shape. The set-up that provided such the selection we described earlier [4, 28]. The discrimination scheme allowed reducing the probability of detecting the gamma radiation photons of a ^{239}Pu-Be source in 10^4 times. The characteristics of a ^{239}Pu-Be source and the method of reconstruction of the neutron spectrum from the measured recoil proton spectrum was described in detail in previous papers [4, 10].

Experimental Samples

We investigated the light yield of single crystals of stilbene ($C_{14}H_{12}$, density $\rho = 1.22$ g/cm^3), anthracene ($C_{14}H_{10}$, $\rho = 1.25$ g/cm^3), and *p*-terphenyl ($C_{18}H_{14}$, $\rho = 1.23$ g/cm^3) [4]. The single crystals of the *p*-terphenyl containing 1,4-diphenyl-1,3-butadiene (0.1% in the melt) as an addition agent were studied as well. All samples had a thickness of 5 mm.

Comparison between Characteristics of the Photoluminescence and the Radioluminescence

Photofluorescence Quantum Yield. Fluorescence spectra were measured by a Varian Cary Eclipse spectrofluoremeter. Basing on these measurements the absolute photofluorescence quantum yield Φ_{ph} of the organic single crystals was calculated. It was obtained that $\Phi_{\text{ph}} = 0.65$ for stilbene, $\Phi_{\text{ph}} = 0.48$ for *p*-terphenyl, $\Phi_{\text{ph}} = 0.97$ for *p*-terphenyl that contains 1,4-diphenyl-1,3-butadiene, and $\Phi_{\text{ph}} = 0.55$ for anthracene.

Radioluminescence Light Yield. The light yield is the total number of photons, which are produced in a scintillator per 1 MeV of particle energy. The light output is that fraction of the light yield of a scintillator which is detected by a photodetector. It is experimentally measured value [4]. The ratio between these values is called the light collection coefficient. Let us denote it as τ_i for excitation of *i*-type. The light collection coefficientτ takes into account geometry of a sample and type of excitation [29].

The light output of organic single crystals we calculated by comparison with the value of the light output for the reference stilbene single crystal. It light yield C was equal to 14,700 photons per 1 MeV of gamma radiation. Table 1 shows the values of the light yield C for the organic single crystals, as well as the values of the light collection coefficients τ_γ, τ_e, and τ_α for the cases of excitation by photons of gamma radiation, conversion electrons and alpha particles, respectively. For the case of the excitation by fast neutrons we used the light collection coefficient identical to that for gamma radiation (τ_γ-value), because for

Table 1. Light yield C and light collection coefficients τ_γ, τ_e, and τ_α of organic molecular crystals

Organic crystal	C, photon/MeV	τ_γ	τ_e	τ_α
Stilbene	14,700	0.659	0.649	0.635
p-Terphenyl (undoped)	17,000	0.576	0.563	0.551
p-Terphenyl (0.1% 1,4-diphenyl-1,3-butadiene)	24,900	0.615	0.608	0.597
Anthracene	29,000	0.596	0.583	0.570

these types of excitation the secondary particle would originate actually in any point of a sample with equal probability.

Energy Yield of the Photo- and Radioluminescence. The photoluminescence energy yield Y_{ph} is defined as:

$$Y_{ph} = \Phi_{ph} \times \frac{\lambda_{ex}}{\lambda_{em}^{av}}, \tag{4}$$

where λ_{ex} and $\lambda^{av}{}_{em}$ are the excitation wavelength and the average wavelength of an emission spectrum, respectively; Φ_{ph} is the absolute photofluorescence quantum yield.

The average value of the RL energy yield for a particle with the initial energy E_0 crossing the maximum range in a scintillator is equal to:

$$\langle Y_r \rangle = \frac{1}{E_0} \int_0^{E_0} Y_r(E)dE = \frac{L}{E_0} \tag{5}$$

where L is the total energy of the RL photons.

Let us use the following notations: $E_{\text{ph}}(\lambda^{av}{}_{em})$ is the average energy of a luminescence photon, E_i is the excitation energy, P_i is the total number of photons in a scintillation pulse, and Y_i is the energy yield. The suffix i means the excitation of i type. Below by ph, γ, e, n, and α we denote the following types of excitation i: light photons, photons of gamma radiation, conversion electrons, neutrons and alpha particles, respectively The symbol of averaging will be omitted. Hence, it is necessary to measure the total number of photons in a scintillation pulse P_i to obtain the value of Y_i for i type of excitation with the energy E_i.

The Number of Scintillation Photons

The following procedure was used to obtain the total number of photons P_i in the RL pulse for i type of excitation. Firstly, we measured amplitude scintillation spectra of organic single crystals obtained for the excitation with the energy E_i. The amplitude scintillation spectra of the samples were measured by a multichannel amplitude analyzer AMA-03F. The analyzer scale was calibrated by the energy lines, which correspond to the edges of the Compton spectra obtained during the excitation by radionuclide sources ^{22}Na, ^{60}Co, ^{137}Cs, and ^{152}Eu. The light output of the scintillators was calculated by the comparison method [29] using the reference stilbene single crystal. After that we recalculated the light yield of the single crystals taking into account the light collection coefficientsτ_γ, τ_e, and τ_α

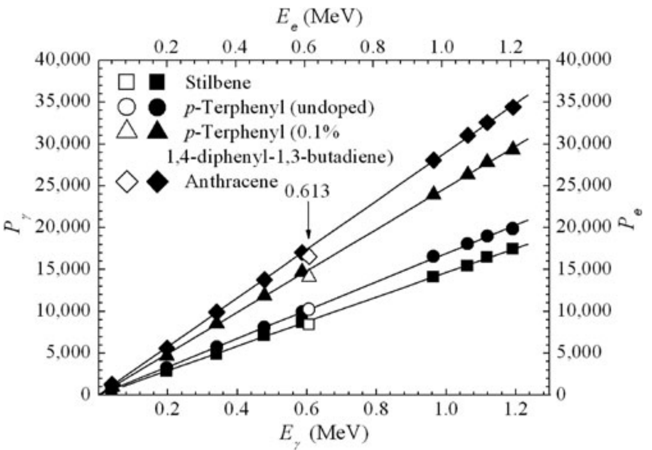

Figure 1. The total number of photons P_γ (closed symbols) and P_e (open symbols) in a scintillation pulse for organic single crystals. The solid lines are the calculated linear dependences of P_γ against E_γ. The arrow indicates the energy $E_e = 0.613$ MeV of the conversion electrons.

(see Table 1). This allowed us to calculate the number of scintillation photons P_i, which are generated in an organic single crystal by the energy E_i.

Figure 1 shows the results of such calculations for the ionizing radiations with low dE/dx. Within the discussed energy range the plot of P_γ as a function of E_γ yields a straight line. For conversion electrons the calculation was performed only for a specific value, which corresponded to the energy of the incident electron E_e. The energy $E_e = 0.613$ MeV corresponds to the experimental conditions. To calculate this value we take into account that before the electron with the initial energy $E_e = 0.622$ MeV strikes a sample it has to pass through a layer of air about 4 cm thick.

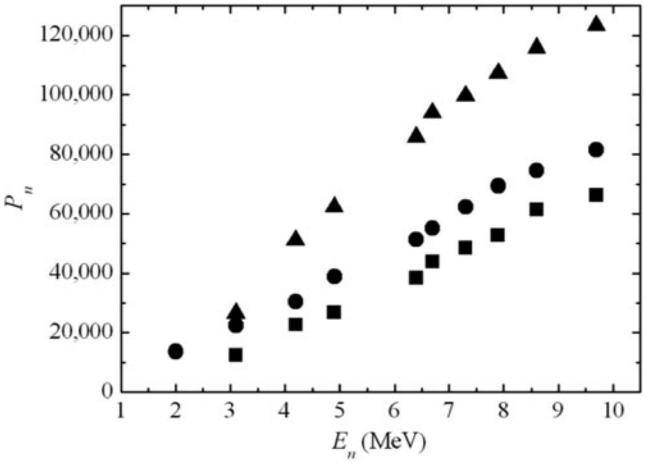

Figure 2. The total number of photons P_n in a scintillation pulse for organic single crystals excited by fast neutrons with the energy E_n. The symbols are the same as in Fig. 1.

Table 2. Values of $E_{\mathrm{ph}}(\lambda^{av}{}_{em})$, Φ_{ph}, and Y_{ph} of organic molecular crystals

Organic crystal	$E_{\mathrm{ph}}(\lambda^{av}{}_{em})$, eV	Φ_{ph}	Y_{ph}
Stilbene	3.08	0.65	0.55
p-Terphenyl (undoped)	3.13	0.48	0.41
p-Terphenyl (0.1% 1,4-diphenyl-1,3-butadiene)	2.88	0.97	0.77
Anthracene	2.71	0.55	0.50

Figures 2 and 3 demonstrate the calculated values of the total number of scintillation photons for molecular single crystals excited by fast neutrons of a ^{239}Pu-Be radionuclide source (values of P_n) and by alpha particles in the energy range from 0.7 to 7.5 MeV (values of P_α), respectively. These dependences obtained for the excitation by the ionizing radiations with high d*E*/d*x* values are non-linear.

Discussion

Low Values of dE/dx

Table 2 presents the values of $E_{\mathrm{ph}}(\lambda^{av}{}_{em})$, Φ_{ph}, and Y_{ph} for the photoexcitation, while Table 3 presents the values of Y_γ and Y_e, obtained for the ionizing radiations with low d*E*/d*x*. The Y_γ-value, according to (5), is equal to the product of a slope of the curve (see Fig. 1) by $E_{\mathrm{ph}}(\lambda^{av}{}_{em})$. The value Y_e is obtained as $P_e \times E_{\mathrm{ph}}(\lambda^{av}{}_{em})/E_e$. In Fig. 1 the values of P_e, practically, are on the corresponding linear dependencies of P_γ against E_γ. Within the energy range of the measurements the interactions of gamma radiation photons with an organic medium are well fitted by Compton effect, which results in generation of secondary electrons [4]. It causes an extremely small difference in parameters Y_γ and Y_e (see Table 3).

The comparison of the data presented by Tables 2 and 3 shows a significant difference between the values of the corresponding parameters obtained for the photoexcitation and the

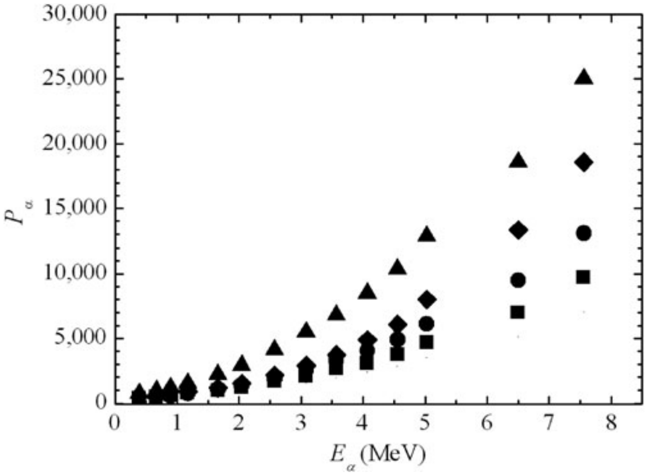

Figure 3. The total number of photons P_α in a scintillation pulse for organic single crystals excited by alpha particles versus the energy E_α. The symbols are the same as in Fig. 1.

Table 3. Values of Y_γ and Y_e of organic molecular crystals

Organic crystal	Y_γ	Y_e
Stilbene	0.045	0.042
p-Terphenyl (undoped)	0.053	0.052
p-Terphenyl (0.1% 1,4-diphenyl-1,3-butadiene)	0.072	0.066
Anthracene	0.079	0.073

excitation by the ionizing radiations with low values of dE/dx. In the case of the excitation by the ionizing radiations with low dE/dx the values of the RL energy yields (Y_γ and Y_e) are by an order of magnitude smaller than in the case of the excitation by light photons of the visible range (Y_{ph}). The question arises "Why?"

In contrast to photoexcitation the generation of molecular excitons in organic crystals by ionizing radiation has a many-stage nature [1, 4, 13, 20, 23]. The decay of a plasmon may lead to generation of a single charge pair. The average energy of a plasmon $\langle E_{\text{pl}} \rangle$ is approximately equal to 20 eV [1, 4, 13, 21, 22]. This value determines the average energy required to generate a single pair of charge carriers. There are at least two other possible reasons those can cause the difference between Y_{ph} and Y_γ or Y_e.

Geminate recombination when an electron recombines with its parent ion results in generation of a singlet exciton [4, 22]. This situation is the most expectable for the spur with one pair. For spurs containing more than one pair the spins of the combining charge states are uncorrelated and random recombination dominates over geminate one [30]. In this case, according to the spin selection rule, S- and T-states occur in the ratio 1 to 3 [4, 7, 19, 30, 31]. Even if we take into account the probability of generation of S-states in the annihilation of T-states then it results in the yield of S-states equal to their yield in the process of geminate recombination taken with the factor ~ 0.4 [31]. Therefore the luminescence yield of the pair recombination decreases. The probability of generation of the spurs with the number of pairs $j > 2$ decreases with increasing j [19].

An escape of an electron from a spur may be the second reason for the energy losses. For the ionizing radiations with low dE/dx the distance between two neighbor spurs is much larger than the size of a single spur, and the possibility of an overlap of spurs is extremely small [4, 19]. Therefore, if an electron escapes from it spur then the probability this electron returns to the parent spur or reaches to a neighbor spur is also extremely small.

So, the RL energy yield for the ionizing radiations with low dE/dx will define by the features of generation and recombination of charge states in separate spurs. These spurs do not overlap. Increasing the particle energy only leads to an increase in the number of such spurs [4, 19]. This explains the linearity of P_γ as a function of E_γ, i.e. the constancy of the light yield as a function of E_γ for the ionizing radiation with low dE/dx (see Fig. 1).

High Values of dE/dx

For fast neutrons and alpha particles we calculated the values $Y_n = P_n \times E_{\text{ph}}(\lambda^{av}{}_{em})/E_n$ and $Y_\alpha = P_\alpha \times E_{\text{ph}}(\lambda^{av}{}_{em})/E_\alpha$, respectively, according to Eq. (5). The Y_n-values for the investigated range of energies E_n and samples of organic single crystals are in the range from 0.012 to 0.040, while in the case of alpha excitation the calculation gives the values of Y_α from 0.0012 to 0.0095. A spread of the values Y_n and Y_α is defined by both a type of

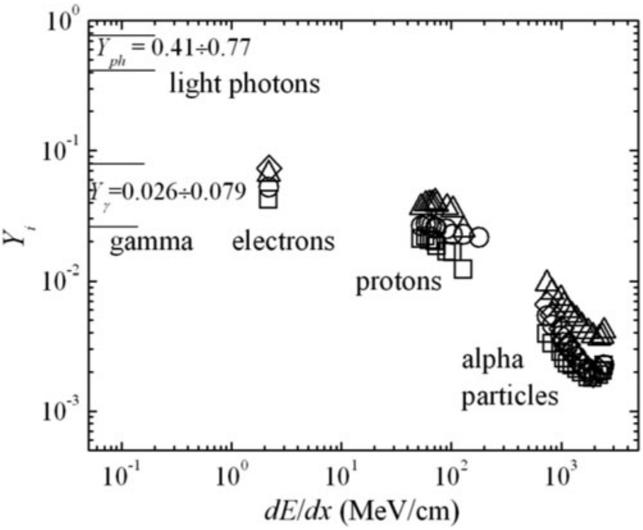

Figure 4. The RL energy yield Y_i of organic single crystals as a function of dE/dx of the ionizing radiation. The symbols are the same as in Fig. 1.

a crystal, and a non-linearity of the scintillation response for the ionizing radiations with high dE/dx.

Figure 4 summarizes the RL energy yields for organic single crystals excited by the ionizing radiations in a wide range of dE/dx. Values of dE/dx were calculated using the online programs ESTAR, PSTAR, and ASTAR of the National Institute of Standards and Technology (NIST) [32]. The range of the Y_{ph}-values (see Table 2), and the range of the Y_{γ}-values (see Table 3) is only indicated in Fig. 4 because the determination of the dE/dx-value is incorrect for these both cases. In the case of neutron excitation we calculated the values of dE/dx for the maximum energy of recoil protons, which were generated by the corresponding fast neutrons with a set of energies E_n.

The complicated dependence of Y_{α} versus dE/dx is caused by a nonlinearity of the light yield as a function dE/dx for high values of dE/dx. With decrease of the energy of an alpha particle, the dE/dx-value increases and reaches a maximum. After that in the end of an alpha particle path Y_{α} grows. The effect of an ion recharge can be the reason of this dependence [4, 33]. According to [33], this effect takes place for alpha particles with the energies about 1 MeV. The same result we have obtained in our measurements.

Figure 4 shows a precipitate drop in the RL energy yield for high dE/dx. For the case of alpha excitation, the Y_{α}-values are 15–30 times less than in the case of the excitations with low dE/dx (the values of Y_{γ} and Y_e). For the ionizing radiations with high dE/dx the overlapping spurs will create the single region of high activation density of the quasi-cylindrical symmetry. This will increase the density of charge state pairs $\mathrm{M_p}^+$ and $\mathrm{M_p}^-$ located at the distances smaller than the radius of the stable polarization surrounding r_{c} (1) of an excess charge carrier. Therefore, the polarization process will accelerate fast random recombination of hot charge states having an excess energy. The probability of a simultaneous recombination of several pairs of hot charge states becomes very high within the small local region of a medium, determined by the value of r_{c}. This will increase the probability of the above-discussed process of a local heating of the track region. The last process will promote an increase in the probability of a non-radiative deactivation of excitation. Such the quenching mechanism, when the light intensity of a single crystal decreases with increasing it heating, is well known as the "temperature" quenching from the photoluminescence investigations [24]. For high dE/dx this effect is significantly stronger and can be a cause of the efficient primary quenching which results in decrease of the RL energy yield Y.

The "concentration" quenching in the particle track is also possible in addition to the "temperature" one. If the concentration of hot charge states drastically decreases during the initial recombination, but still remains high enough, than the secondary stage of quenching is possible. The concentration of S_1-states, which are the source of the fluorescence in the $S_1 \rightarrow S_0 + h\nu$ transition, could be reduced in the processes of the mutual S-S annihilation, S-T annihilation, singlet exciton fission, quenching by doublet states etc. [30].

Conclusion

In contrast to photoexcitation the generation of molecular excitons in organic crystals by ionizing radiations has a many-stage nature. It causes the additional energy losses even for the ionizing radiations with low dE/dx. The main reasons for these losses are caused by: i) random recombination of charge states in a separate spur, ii) an escape of electrons from a separate spur.

The energy losses significantly increase for the ionizing radiations with high dE/dx. Random recombination of hot charge states accelerated by the polarization interaction prevails at high excitation densities. The energy released in the local region, where several pairs of hot charge states recombine, may exceed significantly the energy of S_1-state. This should lead to the mechanism of a radiationless energy deactivation. An efficiency of such energy losses has to grow with increasing dE/dx. The secondary "concentration" quenching of singlet and triplet excitons may increase the quenching effect. Both the processes essentially depend on the concentration of the corresponding states. The secondary quenching takes place after the primary one when the concentration of the states becomes appreciably lower. Therefore the secondary quenching could not have the effect comparable with the effect of the primary quenching.

References

[1] Pope, M., & Swenberg, C. E. (1982). *Electronic Processes in Organic Crystals*, Clarendon Press, Oxford.

[2] Silinsh, E. A., & Capek, V. (1994). *Organic Molecular Crystals: Interaction, Localization and Transport Phenomena*, American Institute of Physics, New York.

[3] Schwoerer, M., & Wolf, H. C. (2007). *Organic Molecular Solids*, WILEY-VCH Verlag GmbH & Co. KGaA, Weinheim.

[4] Galunov, N. Z., & Tarasenko, O. A. (2011). *Ionizing Radiation Track Formation in Organic Condensed Media*, ISMA, Kharkov [in Russian].

[5] Ortmann, F., Bechstedt, F., & Hannewald, K. (2011). *Phys. Status Solidi, Sect. B*, *248*, 511.

[6] Stehr, V., Pfister, J., Fink, R. F., Engels, B., & Deibel, C. (2011). *Phys. Rev., Sect. B*, *83*, 155208.

[7] Birks, J. B. (1967). *The Theory and Practice of Scintillation Counting*, Pergamon Press, London.

[8] Kitaigorodsky, A. I. (1973). *Molecular Crystals and Molecules. Ser.: Physical Chemistry*, 29, Academic Press, New York.

[9] Galunov, N. Z., Seminozhenko, V. P., & Stepanenko, A. M. (2001). *Mol. Cryst. Liq. Cryst.*, *355*, 479.

[10] Budakovsky, S. V., Galunov, N. Z., Karavaeva, N. L., Kim, J. K., Kim, Y. K., Tarasenko, O. A., & Martynenko, E. V. (2008). *IEEE Trans. Nucl. Sci.*, *54*, 2734.

[11] Hull, G., Zaitseva, N. P., Cherepy, N. J., Newby, J. R., Stoeffl, W., & Payne, S. A. (2009). *IEEE Trans. Nucl. Sci.*, *56*, 899.

[12] Kim, H. D., Cho, G. S., & Kim, H. J. (2013). *Radiat. Meas.*, *58*, 133.

[13] Galunov, N., & Tarasenko, O. (2010). *Radiat. Meas.*, *45*, 380.

[14] Galunov, N. Z. (1993). *Mol. Cryst. Liq. Cryst.*, *236*, 121.

[15] Galunov, N. Z. (1994). *Mol. Cryst. Liq. Cryst.*, *252*, 135.

[16] Galunov, N. Z., Jarichkin, V. V., & Tarasenko, O. A. (1995). *Mol. Mat.*, *5*, 189.

[17] Bounds, P. J., Siebrand, W., Eisenstein, I., Munn, R. W., & Petelenz, P. (1985). *Chem. Phys.*, *95*, 197.

[18] Silinsh, E. A., Jurgis, A. J., & Shlihta, G. A. (1987). *J. Mol. Electron.*, *3*, 123.

[19] Mozumder, A. (1999). *Fundamentals of Radiation Chemistry*, Academic Press, San Diego, London, Boston, New York, Sydney, Tokyo, Toronto.

[20] Platzman, R. L. (1962). *Radiat. Res.*, *17*, 419.

[21] Swanson, N., & Powell, C. J. (1963). *J. Chem. Phys.*, *39*, 630.

[22] Schott, M. (1969). *Mol. Cryst.*, *5*, 229.

[23] Fano, U. (1992). *Rev. Mod. Phys.*, *64*, 313.

[24] Kucherov, I. I., & Faidysh, A. N. (1958). *Izv. Akad. Nauk SSSR (Ser. fiz.)*, *22*, 29 [in Russian].

[25] Galunov, N. Z., & Martynenko, E. V. (2008). *Funct. Mater.*, *15*, 380.

[26] Galunov, N. Z., Seminozhenko, V. P., Martynenko, E. V., & Tarasenko, O. A. (2013). *Probl. Atom. Sci. Technol.*, *85*, 210.

[27] Tarasenko, O. A. (2012). *Funct. Mater.*, *19*, 415.

[28] Baker, J. H., Galunov, N. Z., Stepanenko, A. M., & Tarasenko, O. A. (2004). *Radiat. Meas.*, *38*, 817.

[29] Sysoeva, E., Tarasov, V., & Zelenskaya, O. (2002). *Nucl. Instrum. Methods Phys. Res., Sect. A*, *486*, 67.

[30] Geacintov, N. E., Binder, M., Swenberg, C. E., & Pope, M. (1975). *Phys. Rev., Sect. B*, *12*, 4113.

[31] Helfrich, W., & Schneider, W. G. (1966). *J. Chem. Phys.*, *44*, 2902.

[32] NIST Standard Reference Database 124. Stopping-Power and Range Tables for Electrons, Protons, and Helium Ions (http://www.nist.gov/pml/data/star/index.cfm).

[33] Fano, U. (1963). *Ann. Rev. Nucl. Sci.*, *13*, 1.